eLife

Neuroscience

Outer hair cells stir cochlear fluids

Choongheon Lee, Mohammad Shokrian, Kenneth S Henry, Laurel H Carney, Joseph C Holt, Jong-Hoon Nam

Department of Otolaryngology, University of Rochester, Rochester, NY, United States • Department of Mechanical Engineering, University of Rochester, Rochester, NY, United States • Department of Biomedical Engineering, University of Rochester, Rochester, NY, United States • Department of Neuroscience, University of Rochester, Rochester, NY, United States

Reviewed Preprint
v2 • November 12, 2024
Revised by authors

Reviewed Preprint
v1 • October 7, 2024

eLife Assessment

Although others have proposed that OHC electromotility subserves cochlear amplification by acting as a "fluid pump", and evidence for this has been found using electrical stimulation of excised cochleae, this **important** study substantially advances our understanding of cochlear homeostasis. This is the first report to test the pumping effect in vivo and consider its implications for cochlear homeostasis and drug delivery. The manuscript provides **convincing** evidence for OHC-based fluid flow within the cochlea.

https://doi.org/10.7554/eLife.101943.2.sa4

Abstract

We hypothesized that active outer hair cells drive cochlear fluid circulation. The hypothesis was tested by delivering the neurotoxin, kainic acid, to the intact round window of young gerbil cochleae while monitoring auditory responses in the cochlear nucleus. Sounds presented at a modest level significantly expedited kainic acid delivery. When outer-hair-cell motility was suppressed by salicylate, the facilitation effect was compromised. A low-frequency tone was more effective than broadband noise, especially for drug delivery to apical locations. Computational model simulations provided the physical basis for our observation, which incorporated solute diffusion, fluid advection, fluid-structure interaction, and outer-hair-cell motility. Active outer hair cells deformed the organ of Corti like a peristaltic tube to generate apically streaming flows along the tunnel of Corti and basally streaming flows along the scala tympani. Our measurements and simulations coherently indicate that the outer-hair-cell action in the tail region of cochlear traveling waves is for cochlear fluid circulation.

Introduction

The inner ear labyrinth is filled with two lymphatic fluids, the perilymph and endolymph. An electrochemical potential difference between the two lymphatic fluids drives hair-cell mechano-transduction (Fettiplace and Kim 2014). Although the inner-ear fluid system is connected to the

cerebrospinal fluid of the brain through the cochlear and vestibular aqueducts and to the vascular system across the blood-labyrinth barrier, inner-ear fluid is virtually isolated from other body-fluid systems (Salt, Thalmann et al. 1986; Ohyama, Salt et al. 1988). Consequently, intervening in hearing health by delivering substances to the inner-ear fluid through the systemic circulation is challenging. The maintenance of inner-ear fluid composition is achieved locally by the secretion and absorption of ions and molecules through inner-ear epithelial cells (Wangemann and Marcus 2017). As inner-ear fluid homeostasis is maintained locally, a longitudinal electro-chemical gradient exists along the inner-ear labyrinth (Schulte and Schmiedt 1992; Sadanaga and Morimitsu 1995; Hirose and Liberman 2003).

The inner-ear fluid has been reported to be stationary, unlike other lymphatic fluids in the body (Salt and Hirose 2018). Thus, it is considered that substance transport in the inner-ear fluid is governed by diffusion (Salt and Plontke 2005). Diffusion is an effective mechanism for a substance to travel along sub-micrometer distances (Berg 1993). For instance, considering the diffusion speed of small molecules in water, it takes microseconds for neurotransmitters to diffuse across a 20-nm synaptic gap. In contrast, diffusion is inefficient for travel on the centimeter scale. It takes days for a drug applied at the round window to travel 30 mm to the apical end of the human cochlea. In practice, the substance would not reach the apex because it would be resorbed before traveling this distance. Studies on inner-ear drug delivery confirm this principle of physics: Longitudinal mass transport along the inner-ear labyrinth is challenging (Salt, Hartsock et al. 2016; Lukashkin, Sadreev et al. 2020).

The two membranous openings of the inner ear, the oval and round windows, are sites for non-invasive local delivery of substances into the inner ear. Intratympanic injections of antibiotics and anti-inflammatory drugs have been attempted to manage inner ear disorders despite limited efficacy (Lavigne et al. 2016; Salt and Plontke 2018). Releasing a substance at the end of a long, closed tube forms a steep gradient of concentration. Consequently, the substance does not reach distant regions (Salt and Hirose 2018), whereas, in the vicinity of drug release, the concentration is much higher than desired. One remedy is to inject fluid by making two perforations in the inner ear—one for intruding and the other for extruding (Borkholder, Zhu et al. 2014; Tandon, Kang et al. 2016; Talaei, Schnee et al. 2019). Such an invasive approach is often associated with the injection of a substantial fluid volume, larger than the entire perilymph in the inner ear (Szeto, Chiang et al. 2020).

The tube-shaped organ of Corti (OoC) is lined with motile outer hair cells that are activated systematically with a large phase velocity (> a few m/s) toward the apex (Olson, Duifhuis et al. 2012 2011). A previous study suggests that outer hair cell motility can cause oscillatory fluid motion along the triangular fluid channel within the OoC (Karavitaki and Mountain 2007). Recent measurements of OoC vibrations provide a possible explanation for how this longitudinal fluid flow is generated: outer hair cells operate like an area motor by deforming the OoC cross-sectional area (Jabeen, Holt et al. 2020; Guinan 2022; Lin, Macić et al. 2024). Outer hair cells boost the OoC vibrations over the entire span of the traveling waves (Lee, Raphael et al. 2016; Cooper, Vavakou et al. 2018; He, Kemp et al. 2018; Fallah, Strimbu et al. 2019). In theory, peristaltic deformation of the OoC could induce non-oscillatory streaming along the tunnel of Corti (Shokrian, Knox et al. 2020). This peristaltic motion of the OoC has not been explored experimentally.

We hypothesized that outer hair cells agitated by sounds could induce advection of the cochlear fluids. To test this hypothesis, the transport of a neurotoxin along the scala tympani was measured. Kainic acid irreversibly damages afferent synapses with inner hair cells (Sun, Hashino et al. 2001). Importantly, kainic acid does not affect the hair cells, unlike other popular substances used for inner-ear drug-delivery experiments, such as streptomycin and salicylate (Salt, Hartsock et al. 2016; Lukashkin, Sadreev et al. 2020). Kainic acid (10 mM) was administered at the round-window niche in young gerbils. Multichannel electrodes were inserted

into the anteroventral cochlear nucleus (AVCN) to monitor drug effect along the tonotopic axis. The relation between the drug's effect time and location was obtained while controlling sound and activity of outer hair cells, two factors that have not been considered in previous drug-delivery studies. To provide theoretical support for experimental observations, computer models were used to simulate inner-ear drug delivery in three steps: the Virtual Cochlea simulated OoC vibrations due to sound (Zhou and Nam 2019); the Navier-Stokes equation including a nonlinear convective term was solved to obtain the drift of the Corti and scala fluids (Shokrian, Knox et al. 2020); and the diffusion-advection equation was solved to simulate the spatiotemporal change of kainic-acid concentration in the cochlear fluids.

Results

Outer-hair-cell motility and sound properties, such as frequency, level, and bandwidth, were the parameters that we hypothesized to affect drug delivery. Testing these quantities and their combinations requires an extensive series of experiments. In this study, we present a control case and four test cases to focus on two major questions: whether sounds and outer-hair-cell motility affect inner ear drug delivery. The control experiment was the drug delivery in near silence ("Silence"). The test cases included 1) broadband sounds (0.1-12 kHz, 60 or 75 dB SPL) presented during drug delivery ("Sound"), 2) the same broadband sounds presented, but with salicylic acid administered before kainic acid application ("post-SA"), or an 80-dB SPL pure-tone at either 3) 0.5 kHz, ("LF-tone"), or 4) 3-6 kHz ("MF-tone").

Sounds affect inner-ear drug delivery

Before applying 10 mM kainic acid to the intact round window, the characteristic frequencies (CFs) of probing locations were identified (**Fig. 1A, D**). Distortion product otoacoustic emissions (DPOAEs) were measured before and after drug delivery to confirm no change in outer-hair-cell motility during the experiment (**Fig. 1C, F**). When pre- and post-delivery DPOAEs changed more than 5 dB at any frequency between 0.1 and 10 kHz, the results were excluded (four animals). In one set of experiments, over 90% of stimulus intervals were kept silent (approximately 55 seconds per minute, **Fig. 1A-C**). In the other experiments, broadband sounds at a modest level (0.1-12 kHz, 60-75 dB SPL) were played during over 90% of the stimulus intervals (**Fig. 1D-F**). Approximately 8 percent of time (4.6 seconds per minute) were used to acquire background neural activity and to measure responses to 30-40 dB SPL probe tones at three CFs. Under our experimental condition (4 μL of 10-mM kainic acid applied at the intact round window), neural responses were abolished after a few to several hundred minutes (**Fig. 1B, E**). The effect time was defined as the latency following exposure at which the neural response dropped below 75 percent of its baseline value (t_E, **Fig. 1B**). The drug effect was tonotopic, with higher CF locations being affected earlier (**Fig. 1G**). In **Fig. 1H**, the sound- and the silence-case response curves from similar CF locations (between 4.5 and 6.5 kHz) were averaged for comparison. **Fig. 1I** presents the drug delivery data as the effect time (t_E) versus CF location. We acquired 34 data points from 13 gerbils for the sound protocol and 48 data points from 18 animals for the silence protocol. The trend line (broken curve) was obtained by fitting a curve to the silence-case data points with the 1D diffusion equation (Berg 1983).

To compare the effect times of the sound and silence cases despite varying delivery distances, the effect time was normalized by the trend values at respective CF locations and represented in dB (t_E in dB = $20\log_{10}(t_E/t_{Trend})$, **Fig. 1J**). Average t_E over the entire CF range was significantly faster for the sound protocol than for the silent case ($p = 0.0045$). Subsequent analyses of low (<4.5 kHz) and mid-frequency (>4.5 kHz) regions further showed that broadband sound exposure increased the speed of drug delivery in the mid-CF region (> 4.5 kHz, $p < 0.001$) but not the low-CF region (< 4.5 kHz, $p = 0.55$; **Fig. 1K**).

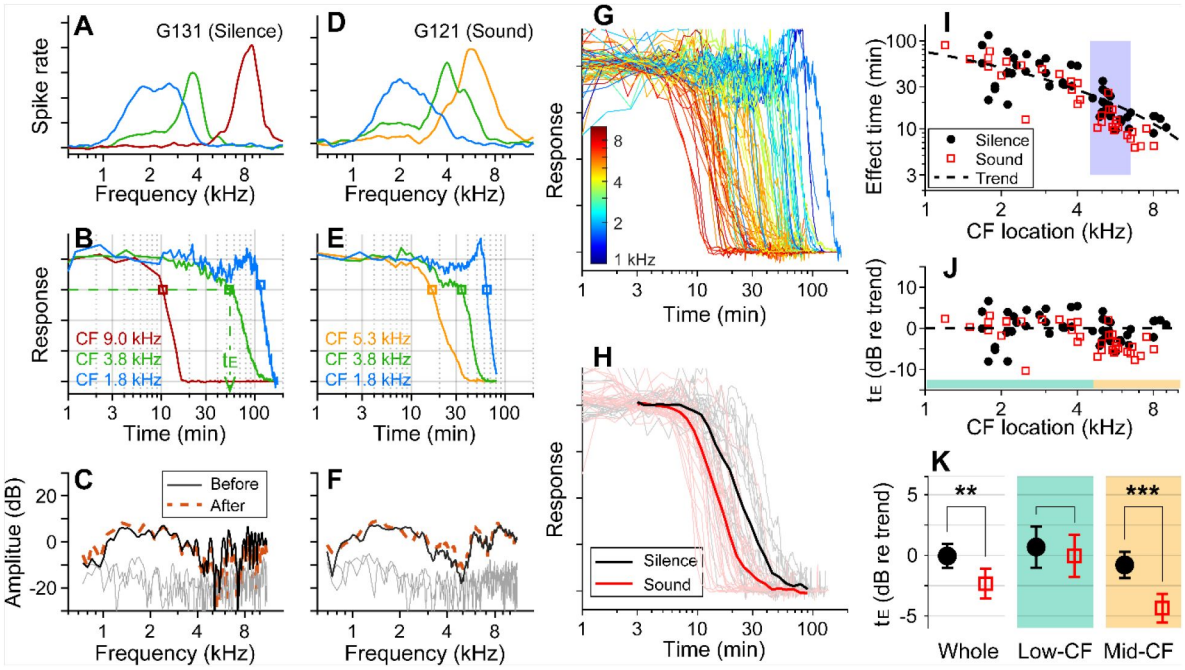

Figure 1.

Sound-facilitated inner ear drug delivery.

Kainic acid was applied to the round window of young gerbils under different acoustic conditions— in silence or with 60-75 dB SPL sounds. (**A**) Tuning curves at 30 dB SPL. The CFs of the three probing channels are 9.0, 3.8 and 1.8 kHz. (**B**) Normalized neural responses in the AVCN versus the time of drug application. The drug effect time, t_E, was defined at the 75 percentiles of normalized curves. In this measurement, it took 54 minutes to affect the 3.8 kHz CF location (green dashed line and arrow). (**C**) DPOAEs were measured before and after the kainic acid delivery. Two stimulating tones were at 40 dB SPL, and the frequency ratio was 1.1. The x-axis is the f_1 frequency. (**A-C**) Example of drug delivered in silence ("Silence" case). (**D, E, F**) Example of drug delivery during the presentation of broadband noise at 75 dB SPL ("Sound" case). (**G**) Response curves with colors representing CFs. Basal (higher frequency) responses decay earlier. Out of 82 measurements, 48 silence-case curves are from 18 animals and 34 sound-case curves are from 13 animals. (**H**) Mean responses of sound and silence cases at similar locations (CF = 4.5-6.5 kHz); n=19 for Silence, and n=13 for Sound. (**I**) Effect time versus CF location. The shaded frequency range corresponds to the data in panel H. The broken curve ("Trend" line) was obtained by fitting a curve to the silence data using 1D diffusion theory. (**J**) Effect time in dB with respect to the trend line. t_E in dB = $20\log_{10}(t_E/t_{Trend})$. (**K**) Two-tailed t-tests between the effect times of sound and silence cases for the entire CF range (whole, n=48, 34 for silence and sound), low-CF locations (<4.5 kHz, n=24, 16 for silence and sound), and high-CF locations (> 4.5 kHz, n=24, 18 for silence and sound).Throughout this paper, the symbols and range bars indicate the mean and the 95% confidence interval, respectively. When an individual data set was presented as an example, the subject identifies are indicated as G###, where ### is a three-digit number.

Outer-hair-cell motility was required for the sound effect

Motile outer hair cells boost cochlear responses to sounds. If the sound effect on cochlear drug delivery depends on fluid agitation from outer-hair-cell motility, inhibiting the motility should produce effect times similar to the silent condition. To test this hypothesis, before delivering kainic acid, salicylic acid was administered intraperitoneally (200 mg/kg) to inhibit outer-hair-cell motility (**Fig. 2A**). DPOAEs were recorded before and after the salicylic acid application to confirm its effect (**Fig. 2B, E**). After salicylate injection, neural responses decayed for 20-30 minutes to reach a steady state (**Fig. 2C, F**). Because the salicylate effect raised the hearing threshold, the probe-tone level was increased by 15-20 dB prior to kainic-acid application (typically from 30 to 50 dB SPL; the discontinuity in the response curve near 70 minutes was due to this increase in the probe tone level).

The red-dashed vertical lines of **Fig. 2C, F** indicate the timing of kainic-acid application. **Fig. 2D** and **G** present only the kainic-acid application responses (the time span after the dashed vertical lines in panels B and E). Note that 75-dB SPL broadband sounds were played in the post-SA protocol. The two examples in **Fig. 2B-G** also demonstrate the variance of the salicylate effect. In one case, DPOAEs decreased by < 10 dB (re: 40 dB stimulation) and the neural responses to 30 dB SPL sound decreased by 40 percent (**Fig. 2C**). In the other case, DPOAEs decreased by approximately 20 dB, and the neural responses to 30 dB SPL sound decreased to the noise floor (**Fig. 2F**). For the post-SA protocol, we acquired 24 data points from 8 animals. The post-kainate response decay of salicylate-treated ears followed the trend of the silence case despite use of the sound protocol (**Fig. 2H**). Despite the sound stimulation, the effect time of the post-SA case was not different from the silence case ($p = 0.096$) and was greater than the sound case ($p < 0.001$, **Fig. 2J**). Like the silence versus sound protocols comparison, the statistical difference was from the mid-CF locations, not from low-CF locations (**Fig. 2J**). The post-SA results support the hypothesis that outer-hair-cell motility is required for faster inner-ear drug delivery with sound exposure.

Low-frequency tones were more effective

If the sound effect on cochlear drug delivery were due to fluid agitation, other sounds might be more effective than random noise. Vibrations along the cochlear partition propagate with decaying phase velocity toward the apex, before stalling shortly after reaching the sound's CF location. Advective flow of the cochlear fluid is shaped by the vibration frequency and amplitude and by the phase velocity of traveling waves (Lighthill, 1993; Shokrian, Nam, 2020). To test the hypothesis that the type of sound stimulus impacts the effectiveness of drug delivery, especially in low-frequency regions, pure-tones at 80 dB SPL were played during inner-ear drug delivery, instead of broadband noise. In choosing the frequency of the pure tone, we considered the nature of cochlear traveling waves, guided by fluid-dynamics simulations (Zhou and Nam 2019; Shokrian, Knox et al. 2020). The frequency of 0.5 kHz was chosen close to the low bound of the gerbil's audible frequency range. The mid-frequency was selected from between 3 and 6 kHz to match the CF location of one of the electrode probes. If the sound facilitation were most prominent near the peak of traveling waves, the low-frequency tone would be inefficient in facilitating drug delivery to high-to mid-CF locations. Whereas, if the phase velocity were crucial for fluid agitation, the low-frequency sound should be advantageous because of its long tail region with high phase velocity. If the traveling wave pattern set the cochlear fluid flow, the sound-facilitation effect could stall at one location, similar to the traveling waves.

With the pure-tone protocol, 45 data points were acquired from 15 gerbils. In two example cases, the effect time at low-CF locations (CFs near 2 kHz) was 15 minutes for the case of the 0.5 kHz tone (**Fig. 3A**) and 100 minutes for the 3.5 kHz tone (**Fig. 3B**). In the mid-CF locations, the effect time did not differ for different tone frequencies: the effect time ranged between 8 and 12 minutes for CF locations between 5.9 and 6.3 kHz (red curves of **Fig. 3A, B**). In some cases, especially toward the low-CF locations, the response curve had bimodal decay patterns (e.g., the cyan curve

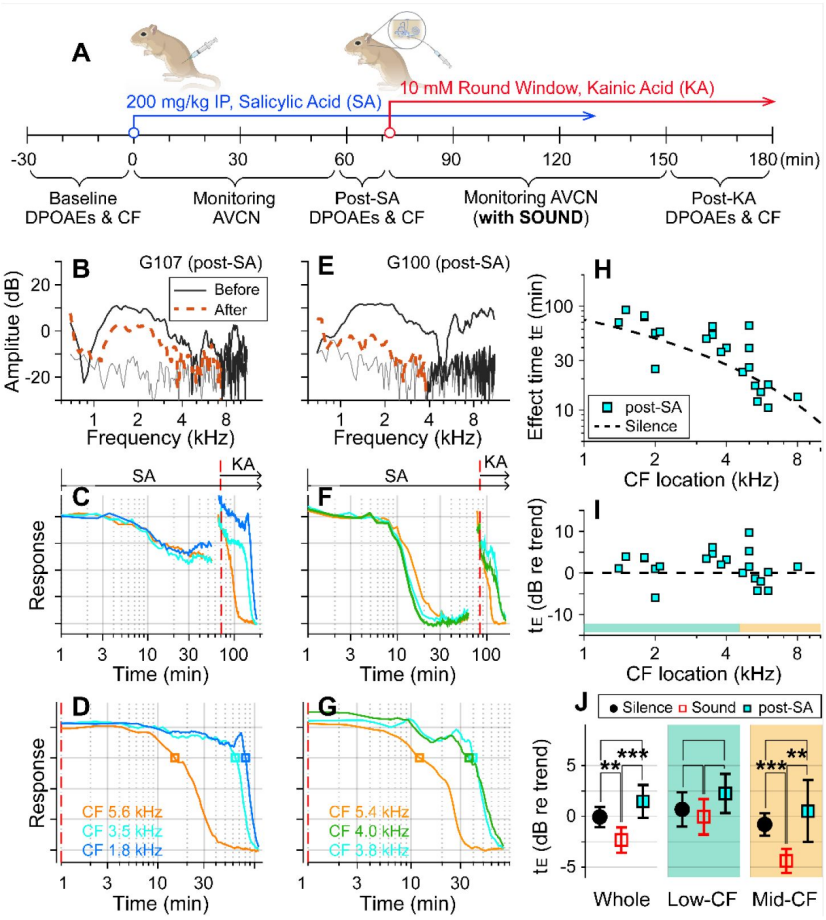

Figure 2.

Suppressing motility of outer hair cells by salicylate.

(**A**) Under the "post-SA" protocol, salicylic acid (SA, 200 mg/kg) was administered IP before applying kainic acid at the round window. Broadband noise at 75 dB SPL was played during experiments. (**B**) DPOAEs before and after salicylic acid and kainic acid delivery. (**C**) Overall response curves. IP salicylic acid was administered at t=0. The red vertical line indicates when kainic acid was applied to the round window. The arrows indicate the application spans of salicylic acid (SA) and kainic acid (KA). (**D**) Normalized neural responses after kainic-acid application (the curves after the red line in panel B). (**E, F, G**) Another example of the post-SA protocol. (**H**) Effect time versus CF location of post-SA measurements (n=22 from 8 animals). The silence-case trend line is the same as **Fig. 1**. (**I**) The effect time in dB with respect to the trend line. (**J**) Two-tailed t-tests between the effect times of sound, silence, and post-SA cases for the entire CF range (whole), low-CF locations (<4.5 kHz, n = 12 for the post-SA case), and high-CF locations (> 4.5 kHz, n=10 for the post-SA case).

in **Fig. 3B**), resulting in a broader distribution in the effect time. The overall plots of effect time versus location (**Fig. 3C, D**) show that most data points are below the trend line of the control (silence) case. That is, the pure-tone stimulation facilitated the delivery throughout the cochlea. According to the statistical analysis of effect time differences between the silence and the pure-tone protocols (**Fig 3E**), low-frequency tones facilitated the drug delivery for both low-($p < 0.001$) and mid-CF locations ($p = 0.011$). Mid-frequency tones facilitated for mid-CF locations ($p < 0.001$) but not significantly for low-CF locations ($p = 0.084$). Low-frequency tones were more effective than broadband noise especially at the apical low-CF locations (**Fig. 3F**, $p < 0.0005$ for all CF locations, $p < 0.00001$ for apical locations with CF < 4.5 kHz).

Figure 4 summarizes our findings for all four cases—control (delivery in silence, **Fig. 4A, B**), sound (broadband noise at 60 or 75 dB SPL, **Fig. 4C, D**), post-SA sound (SA applied intraperitoneally (IP) or to the round window 30-40 min before kainic-acid application, broadband noise at 75 dB SPL, **Fig. 4E, F**), and pure-tone sound (either 0.5 kHz or 3-6 kHz at 80 dB SPL, Fig. G, H). The broken trend lines shown in all panels are the same, obtained by a curve fit to the control (silence) data using the 1D diffusion equation. Broadband sounds decreased the effect time in the mid-CF locations (CF > 4.5 kHz) but had little effect in the low-CF locations (CF < 4.5 kHz, **Fig. 4C, D**). While measurements at two levels (60 and 75 dB SPL) were pooled in **Fig. 1**, they are distinguished in **Fig. 4C** and **D**. Although the mean effect time of the 75 dB SPL data was smaller than for 60 dB SPL in the mid-CF region, supporting the sound-facilitation hypothesis, a larger sample number will be required to confirm the effect of sound level. The sound effect disappeared after inhibiting outer-hair-cell motility with salicylate (**Fig. 4E, F**). In **Fig. 2**, only IP-administered data of the post-SA case are presented. **Fig. 4E** and **F** include additional data on the local (round-window) application of salicylate before applying a solution containing 10 mM kainic acid and 100 mM salicylic acid. While the local-delivery case reduced the mean effect time in the mid-CF region, the effect times of both post-SA cases were not significantly different from the control case. For the mid-CF region, the difference in mean effect time between the two post-SA cases was ascribed to the incomplete inhibition of outer hair cells in the local-delivery case. The most prominent effect was observed when the drug was delivered while playing a low-frequency tone. For instance, 17 out of 18 effect times for the LF-tone case (red square symbols, **Fig. 4G** and **H**) were below the trend line of the control (silence) case.

The mechanism of sound facilitation for drug delivery

was investigated with computer model simulations. Our computer model is distinguished from most cochlear mechanics models in three aspects. First, it incorporates the interactions between the Corti fluid and OoC structures. Second, the nonlinear advection term in the Navier-Stokes equation was not neglected. Finally, both diffusion and fluid advection were considered. Our simulated results support the hypothesis that the cross-sectional area change of the OoC performs like a peristaltic pump (i.e., active outer hair cells are the fluid pumps) (Shokrian, Knox et al. 2020). **Fig. 5** shows half of the cochlear fluid space—the scala tympani and the OoC fluid spaces (omitting the scala media and scala vestibuli). We simulated two cases: In the silence case, the drug delivery was purely governed by diffusion (**Fig. 5A**). In the LF-tone case, both diffusive and advective mass transports contributed (**Fig. 5B-D**). For the LF-tone case, a 1-kHz tone at 80 dB SPL sound was played continuously. The contours in **Fig. 5A** and **B** represent the concentration of the substance at 30 minutes after the onset of delivery. As expected from Fick's law and the log-scale plots of **Fig. 4**, the gradient over distance decays logarithmically. That is, contour lines in **Fig. 5A** have similar spacings in the log scale. However, such a logarithmic gradient was apparently disturbed between the 0.1 and 0.01 mM contour lines in **Fig. 5B**. The contour line is stretched toward the right (red double-headed arrow) in the top Corti fluid layer and to the left (blue arrow) in the bottom scala fluid layer. This stretched contour line was due to the advective flow. In **Fig. 5C** and **D**, the contour lines represent the streamlines (i.e., particles would drift along the contour lines). The red and blue colors indicate clockwise and counterclockwise circulation, respectively. **Fig. 5D** presents the fluid streaming near the peak of

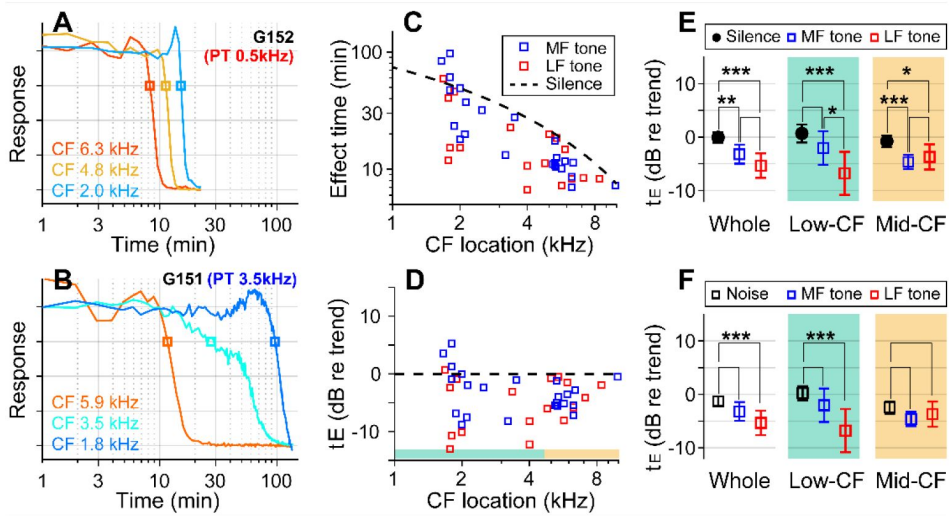

Figure 3.

Pure tones yield shorter effect times than broadband noise.

(**A**) Drug delivery during presentation of a tone at low-frequency (0.5 kHz 80 dB SPL) or (**B**) mid-frequency (3.5 kHz 80 dB SPL). (**C**) Effect time of drug delivery under the low- and mid-frequency tones. The trendline of the silence case is the same as **Fig. 1I**. n = 18 from 6 animals for LF tone. n = 22 from 8 animals for MF tone. (**D**) Normalized effect time. (**E**) Statistical comparison between the three cases (silence, low- and mid-frequency-tone protocols). The two-tailed t-tests were performed on all CF locations, low-CF (< 4.5 kHz, n = 12, 9 for MF- and LF-tone) and high-CF (> 4.5 kHz, n = 10, 8 for MF- and LF-tone) locations. (**F**) Normalized effect time under three sound-conditions compared: Broadband noise, mid-frequency-tone and low-frequency-tone.

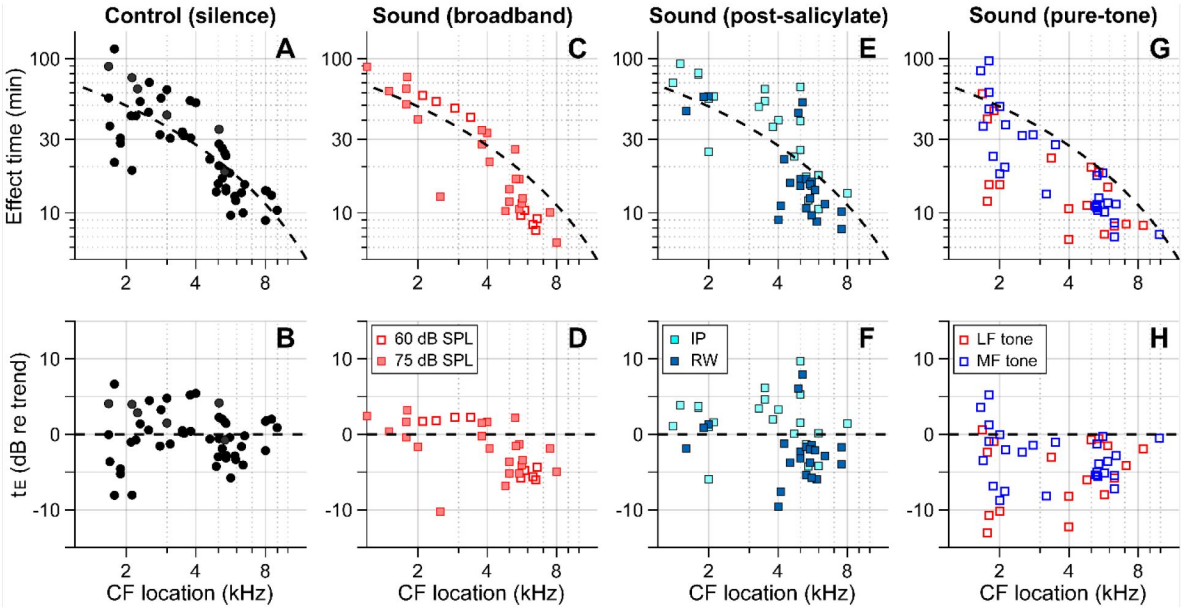

Figure 4.

Outer-hair-cell motility facilitates inner-ear drug delivery.

Summary of the effects of different acoustic and physiological conditions on inner-ear drug delivery. The y-axes represent absolute effect time in minutes (top) and relative effect time in dB w.r.t the trend line (bottom). The same trend line (broken lines, obtained from the control case) is presented for all panels. (**A, B**) Effect time in silence. (**C, D**) Effect time under 60 or 75 dB SPL broadband (0.1-12 kHz) sounds. (**E, F**) Effect time when outer-hair-cell motility was suppressed by salicylate. Before kainic acid application, the salicylic acid solution was administered systemically (intraperitoneally-IP, 200 mg/kg) or locally (round window-RW, 10 mM). (**G, H**) Effect time under 80 dB SPL pure tones. A 0.5 kHz (low-frequency-LF) or 3-6 kHz (mid-frequency-MF) tone was presented during drug delivery. The mid-frequency tone was chosen to match one of the probe frequencies.

the traveling wave (6-9.5 mm from the base, Corti fluid and top 120 μm-thick scala fluid). The maximum streaming velocity is as substantial as a few mm/s. Our simulation shows that active outer hair cells generate a strong stream toward the apex along the tunnel of Corti. The displaced fluid in the apex flows toward the base along the bottom of the scala tympani. The strong advection takes place in the tail of the traveling wave, over a few mm.

Discussion

We showed that sound exposure increases drug delivery from the round window to apical cochlear locations. Sound-facilitated drug delivery was compromised when outer-hair-cell motility was inhibited. Low-frequency tones were more effective than broadband noise in delivering substances to the apex of the cochlea. These results not only highlight new strategies for improving drug delivery throughout the cochlear spiral, but reveal a new function of outer hair cells, beyond sound amplification.

Neural responses near CF are amplified, showing enhanced tuning. In contrast, outer hair cells boost the vibrations in the OoC non-selectively (Cooper, Vavakou et al. 2018; He, Kemp et al. 2018; Fallah, Strimbu et al. 2019). To reconcile the nonselective input (untuned OoC vibrations) and the selective output (tuned neural signals), previous studies suggest that outer hair cells accumulate their power along cochlear traveling waves, referred to as global amplification (Zagadou and Mountain 2012; He, Burwood et al. 2022). However, experimental evidence is incongruent with the global amplification theory (Fisher, Nin et al. 2012; Versteegh and van der Heijden 2013; Dewey, Applegate et al. 2019). According to the two-tone suppression experiment of Dewey et al. (2019), the suppression of outer hair cells far basal from the CF location does not affect the response at the CF location. Available evidence shows that the amplification due to outer-hair-cell action occurs between a location one half-octave basal to the peak and the peak location (Dong and Olson 2013; Fallah, Strimbu et al. 2019). The present study provides new insights into the nonselective outer hair cell action.

Broadband action of outer hair cells helps cochlear-fluid circulation. Our pure-tone experiments (**Fig. 3**) and simulation (**Fig. 5**) show that the region of sound-facilitated drug delivery spanned regions far basal to the CF location of a given sound frequency. Such sound facilitation disappeared when outer hair cell motility was suppressed (**Figs. 2**), which implied that active outer hair cells are the stirrers in the cochlea that drive lymphatic-fluid circulation. From an evolutionary perspective, mammals stretched their hearing organ to encode broader bandwidth with good frequency resolution. The longer cochlea might have entailed a challenge: Maintaining the freshness of the stationary lymph along a long and narrow tube is nontrivial. For instance, a local failure in homeostasis could cascade along the cochlea, making the system vulnerable to disturbance or trauma. The OoC in the basal cochlea suffers from a maintenance burden: a greater influx of potassium (greater MET current) and a smaller clearance surface. We hypothesize that the longitudinal circulation of lymphatic fluid serves as a protective mechanism for the fluid homeostasis of the mammalian cochlea. One potential implication is that an acoustically rich environment could be beneficial in maintaining healthy hearing as well as recovering from damaged hearing.

Our study complements existing studies regarding cochlear fluid homeostasis and differs from previous studies in several ways. The intrastrial fluids (extracellular fluids in the stria vascularis) have been more thoroughly investigated because the three layers in the stria vascularis (marginal, intermediate, and basal cells) maintain the endocochlear potential (Wangemann 2006). Equilibrium in the Corti fluid has been sparsely investigated because its electrochemical gradient is modest compared to that of the intrastrial fluids (Johnstone, Patuzzi et al. 1989; Zidanic and Brownell 1990). Local electrochemical balance in the cochlear fluids has been considered within a radial section (Quraishi and Raphael 2008; Patuzzi 2011; Nin, Hibino et al. 2012). Our study

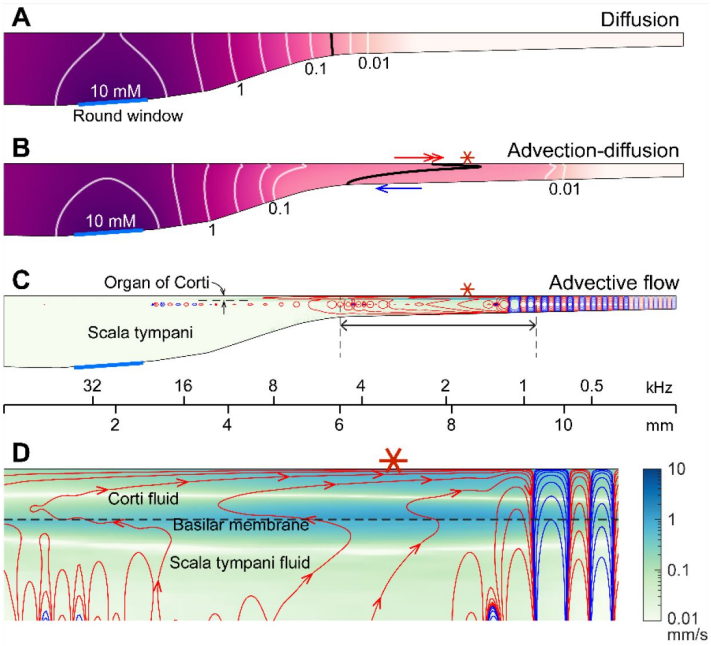

Figure 5.

Active outer hair cells drive fluid flow.

Inner-ear drug delivery was simulated using a computational model. (**A**) Drug delivery due to diffusion. The concentration profile over the cochlear length at 30 minutes after drug application to the round window. (**B**) Drug delivery with 80 dB SPL, 1-kHz sound. The black contour line demonstrates how advection affects drug delivery. (**C**) Steady-state drift flow of the cochlear fluids. Red and blue curves represent the clockwise and counterclockwise streamlines. (**D**) The region with the fastest advection. The drift velocity (green color contour) is as large as a few mm/s.

is focused on the longitudinal (global) equilibrium along the cochlear coil and did not consider the equilibrium across the stria vascularis cell layers. To examine whether the longitudinal fluid flow driven by outer hair cells is strong enough to affect cochlear fluid homeostasis, future studies should measure the K^+ equilibrium and recycling along the length of the Corti fluid under sound and silence conditions.

The nature of the streaming pattern supports the feasibility of targeted inner-ear drug delivery. Two characteristics implicated in the pure-tone experiments (**Fig. 3**) became apparent in the model simulations (**Fig. 5**): the advection caused by active outer hair cells created a 'fast track' and a 'stalling point' for mass transport. For instance, the span between locations 5.5 and 9 mm is the fast track of mass transport (the arrows of concentration contours in **Fig. 5B** and the clockwise advective flow in **Fig. 5C**). In this fast track, the distance between contour lines is much larger than the other regions or the pure diffusion case. The contour line in the fast track (black curve, **Fig. 5B**) is stretched toward the apex in and near the Corti fluid and toward the base at the bottom of the scala tympani, indicating longitudinal fluid circulation. In contrast to the fast-track region, there was a stalling point where the transport stopped. The stacking contours near 10 mm in **Fig. 5B** are caused by the countering circulation loops at 9 mm in **Fig. 5C**. Taking advantage of these 'fast tracks' and 'stalling points', one could design a sequence of sounds to deliver a substance from the round window to a targeted location in the cochlea.

Further work is needed before our findings can be used to address practical problems. Although we showed that low-frequency tone is superior to a high-frequency tone or a broadband sound in facilitating inner ear drug delivery, we have not identified the optimal delivery scheme. While the gerbil cochlea is a better model to study longitudinal mass transport compared to the shorter mouse cochlea (12 mm versus 6 mm), substantial extrapolation is inevitable to predict drug delivery in the 34-mm-long human cochlea out of the present results. Extensive experiments would be needed to examine different sound pressure levels at different frequencies and their combinations in a longer cochlea. Guidance from reliable theoretical models will help to design more efficient experiments and to interpret measured data more rigorously. Our present computer model incorporated the nonlinearity in advection-diffusion dynamics but did not implement the compressive nonlinearity of the sensitive cochlea. To analyze cochlear mass transport under stimulation by complex sounds, a model must address a long list of physical and physiological problems: deformable OoC, Corti fluid dynamics, nonlinear hair cell mechano-transduction, outer-hair-cell motility, permeable basilar membrane, nonlinear fluid dynamics including advection, diffusion solved simultaneously with advection, and the electrochemical equilibrium across the OoC. Our present model includes the essential components of these, but some are extensively simplified (e.g., outer-hair-cell motility, basilar membrane permeability), and some are absent (e.g., hair-cell nonlinearity, electrochemical equilibrium).Fortunately, there are other theoretical models that represent these aspects of cochlear physics and physiology that are lacking in our present study.

Materials and Methods

Experimental approach

Animal Preparation

Sixty-four Mongolian gerbils (*Meriones unguiculatus*, 25 males and 39 females, Charles River Laboratories) were 2-3 months of age. All experimental procedures were in accordance with NIH guidelines and approved by the University of Rochester Animal Care and Use Committee. Animals were anesthetized with an IP injection of ketamine (140 mg/kg) and xylazine (6 mg/kg) and placed on a closed-loop heating pad to maintain body temperature at 37 ± 0.5 °C. Ketamine and xylazine

were then administered continuously through a subcutaneous catheter at a baseline rate of 85 and 3.5 mg/kg/hr, respectively, and adjusted as needed to maintain an areflexic state. Supplemental IP injections of ketamine and xylazine were occasionally administered as required. A tracheotomy and intubation ensured an open airway. Breathing rate was monitored using a thermistor placed in front of the trach tube. The right pinna was removed, and the bulla was exposed. A hole made in the dorsal and caudal bulla allowed access to the temporal bone and round window. After securing the skull using dental acrylic, customized headpost and ear bars, and a stereotaxic frame (Kopf Instruments, Model 900), a craniotomy was made in the temporal bone for electrode penetration through the dura to the AVCN (for details, Frisina, Chamberlain et al. 1982). The head was oriented with the nose pitching downward at 45 degrees so that the round window niche faced upward to better contain the pharmaceutical solution.

Drugs used

Pharmacological agents included the kainic receptor agonist kainic acid (Abcam and Tocris) and sodium salicylate (Sigma-Aldrich). A 10-mM kainic acid solution (volume of 4 µL) was applied at intact round-window niche. The kainic acid solution was prepared in Hank's balanced salt solution (HBSS, Sigma-Aldrich). No discernible effects of different solvents on the AVCN responses were observed (data not shown). Sodium salicylate was dissolved in HBSS for local round-window delivery at a concentration of 100 mM (volume of 4 µL) or dissolved in saline for IP injection at a dose of 200 mg/kg (volume of 0.3 mL).

Measurement protocol

All experiments were performed in a soundproof chamber. A pair of speakers and a microphone (ER-2 and ER-10, Etymotic) were plugged and sealed into the ear canals through a coupler. The sound pressure level (SPL) in the ear canal was calibrated between 0.1 and 16 kHz. A reference electrode was inserted into the muscles of the back of the neck. A multi-channel electrode (Q1×4-10mm-100-177-EIB, Neuronexus or ASSY-37 Fb Acute 32 channel, Cambridge Neurotech) was advanced 2-3-mm into the AVCN using a hydraulic microdrive (Model 640, Kopf Instruments), with a rostro-caudal angle between 60-65 degrees and lateral angle between 40-50 degrees with respect to the interaural line. The characteristic frequencies (CFs) of the four multi-unit channels were identified using tones.. Typically, three channels were identified showing well defined frequency tuning and distinct CFs (**Fig. 1A, D**). Neural responses were amplified and bandpass filtered between 0.75-10 kHz, then sampled (National Instruments PCIe-6251, 50 kHz or Intan RHD 2000, 30 kHz) for storage on a computer hard drive. Neural recordings were transformed with a Teager energy operator to enhance spiking activity (Choi et al., 2006) and the average value of the Teager-transformed response waveform was taken as a measure of the neural response amplitude. Typical time courses of neural signals are shown in **Fig. 1C** and **F** (kainic acid was administered at t = 0). Experiments lasted between 1 and 3 hours.

Drug solutions were applied either at the intact round window niche using a 100 µL Hamilton syringe or through IP injection. After experiments, it was confirmed that the solution was still contained in the round window niche. While kainic acid diffused into the cochlea, the neural signals from the AVCN were recorded under three acoustical conditions: For the "Sound" protocol, 1.1-s noise pips (60-or 75-dB SPL, 0.1-12 kHz bandwidth, 0.8-s duration including 0.15-s onset/offset ramps) were presented continually. After 48 noise pips, one 1.1-s silent pause and three CF tone pips followed (a total of 51 pips and a pause make a 57.2-s sequence). The CF tone pips were presented at the level of 35 dB SPL to monitor neural responses. The silence pause was to monitor spontaneous neural responses. The sequence was repeated until neural signals at the lowest CF site were completely abolished. The neural responses presented in this study are the 'driven responses' obtained by subtracting the spontaneous responses from the responses to the 35 dB CF tones. For the "Silence" or "Pure-tone" protocol, the noise pips of the Sound protocol were replaced with either silence pauses or a pure tone at 80 dB SPL. The pure tone frequency was either 0.5 kHz or a frequency between 3 and 6 kHz matching one of the mid-frequency probe channels. Stimuli

were generated in Matlab (50-kHz sampling frequency), converted to analog (National Instruments PCIe-6251), adjusted to the desired level using analog attenuation (PA5; Tucker Davis Technologies, Alachua, FL), and presented using a headphone buffer amplifier (HB7; Tucker Davis Technologies).

Distortion product otoacoustic emissions (DPOAEs)

DPOAEs before and after the kainic acid delivery measurement were used to confirm that outer hair cell function did not change (**Fig. 1C, F**). DPOAEs were recorded in response to swept primary tones, f_1 and f_2, with f_2 increasing linearly from 0.5 to 10 kHz over 4 seconds, and $f_2 = 1.25\ f_1$. Primary tones (4.05-s duration including 25-ms raised-cosine on/off ramps, with 300-ms inter-stimulus intervals) were presented from separate earphones with equal sound levels, from 40-70 dB in 10-dB steps. DPOAEs were amplified by 40 dB prior to sampling and were averaged across 10 stimulus presentations. DPOAE level at $2f_1$-f_2 was estimated using a least-squares fitting procedure (Long et al., 2008) in Matlab, based on a 100-ms Hann window shifted in 20-ms steps (Wong et al., 2019). The same analysis was applied to a 'null' response, computed as the difference between average even and odd-numbered stimulus presentations, to determine the noise floor.

Modeling approach

Cochlear fluid dynamics were divided into three sequential stages. Different assumptions were used in each stage to represent the relevant physics appropriately and to make the computational analyses affordable. First, OoC vibration due to sound stimulation was estimated by solving fluid-structure interactions between scala fluids, the Corti fluid (extracellular fluid in the OoC) and the OoC. The active feedback from outer-hair-cell motility was incorporated into OoC mechanics. Second, the drift velocity of the fluids in the OoC and the scala tympani in response to OoC vibrations was computed. Drift velocity originates from the nonlinear convective term in the governing equations for the incompressible flow (ref Shokrian et al 2020). The spatial resolution required to evaluate the drift velocity made this stage computationally costly. Unlike the first stage, the advective component of fluid motion was incorporated. The OoC vibrations obtained at the first stage were given as kinematic boundary conditions in this second stage. The fluid motion within the OoC, as well as in the scala tympani, was computed. Third, the spatiotemporal pattern of substance concentration due to advection and diffusion was obtained. The drift velocity field obtained in the second stage was the input for this third stage. The first and second stages were simulated using custom-written Matlab programs, while the third stage was solved using commercially available software (COMSOL multiphysics).

OoC vibrations

The OoC complex structures were discretized into 3-D finite elements reflecting anatomical details. For instance, each hair bundle, hair cell, Deiters cell, or pillar cell was represented by a fully deformable beam. The tectorial and basilar membranes were presented by a meshwork of beams. Their mechanical properties were determined either by using known values or by comparing them with existing mechanical measurements (Nam and Fettiplace 2010; Liu, Gracewski et al. 2017; Marnell, Jabeen et al. 2018). Mechano-transduction kinetics of hair bundle and outer-hair-cell electromotility were incorporated with the OoC finite-element model (Nam and Fettiplace 2012; Nam 2014). The scala-fluid domain was discretized into linear quadrilateral elements. The scala-fluid pressure was determined by two vibrating boundaries—one is the oval window, and the other is the OoC complex. In turn, the OoC structures vibrate due to differential pressure across the OoC

Drift velocity of fluids

From the round window to the inner hair cell, kainic acid molecules travel (drift) across two fluid spaces separated by the basilar membrane: 1) the Corti fluid, and 2) the scala-tympani fluid. The Corti fluid includes the fluid in the tunnel of Corti, Nuel's space, gaps between outer hair cells, and

the outer tunnel. These sub-spaces are interconnected to one another by a few micrometer gaps. For simplicity, the 3-D fluid spaces were reduced to 2-D after reducing the radial dimension. The top boundary of the 2-D Corti fluid was modeled as a deforming wall while the bottom surface shared with scala tympani was implemented as a permeable boundary representing the basilar membrane. The OoC deformation was represented by the relative motion between the top and bottom surfaces of the Corti fluid. The pressure (p) and velocity ($\mathbf{u}$) of the incompressible fluid were determined by the Navier-Stokes and continuity equations.

$$\frac{\partial \mathbf{u}}{\partial t} + \mathbf{u} \cdot \nabla \mathbf{u} = -\frac{1}{\rho}\nabla p + \nu \nabla^2 \mathbf{u}, \text{ and} \tag{1}$$

$$\nabla \cdot \mathbf{u} = 0, \tag{2}$$

where ν and ρ are the kinematic viscosity (70×10^{-6} m^2/s) and density (1 g/cm^3). Note that this viscosity value is a hundred times the value of the water after Prodanovic et al. (2019). The second term in Eq 1 representing advection renders this equation nonlinear. This term has been neglected in cochlear mechanics studies because it hardly contributes to forming the cochlear traveling waves. However, for the purpose of this work (to investigate cochlear mass transport due to advection), this term had to be incorporated despite the increased computational cost. The basilar membrane was considered to have finite permeability using Darcy's law. The fluid velocity passing through the basilar membrane (u_p) is proportional to the transmembrane pressure difference Δp), or

$$u_p = -K\Delta p. \tag{3}$$

The value of the permeability coefficient, K, of 1 m/(sPa) was empirically determined so that the Corti-fluid pressure level was not excessive (< a few Pa). Preliminary simulation results showed that drift velocities were not sensitive to the chosen value of K, even over an order of magnitude from the chosen value. Because of the basilar membrane's permeability, in general, the fluid velocity just above or below the basilar membrane (u_f) is different from the basilar membrane velocity (u_m) by u_p, or

$$u_f = u_m + u_p. \tag{4}$$

When periodic stimulation was applied, the resulting fluid motion was also periodic. Albeit much smaller than oscillatory motion, there existed non-periodic fluid motion that made fluid particles drift over time. When fluid motion is integrated over a period, T, the oscillatory component cancels out, leaving only drift. The drift velocity $\mathbf{u}_D$ at position $\mathbf{x}_p$ and time $t + 0.5T$ was computed as

$$\mathbf{u}_D(\mathbf{x}_p, t + 0.5T) = \frac{1}{T}\int_t^{t+T} \mathbf{u}_E(\mathbf{x}_p, \tau)d\tau, \tag{5}$$

where $\mathbf{u}_E$ is the Eulerian velocity obtained as a solution of the Navier-Stokes equations.

Diffusion

Mass transport is governed by the advection-diffusion equation.

$$\frac{\partial C}{\partial t} = D\,\nabla^2 C - \mathbf{u}_D \cdot \nabla C, \tag{6}$$

where C is the concentration of the transported substance and D is the diffusion coefficient. The whole fluid domain is impermeable (or $\partial C/\partial n = 0$, n is the vector normal to the surface) except for the round window and the basilar membrane. At the round window, the concentration level was constant at 10 mM. The effect time at a specific location was defined as the time to reach 1% of the round-window concentration (100 μM).

Computation

The mesh for the fluid dynamics model (the first stage, Eqs. 1 and 2) consisted of approximately 25,000 second-order quadrilateral elements with the same degrees of freedom for both velocity and pressure. The grid size of the mesh was determined considering the boundary layer thickness of $(\nu/\omega)^{0.5}$, where ω was the highest frequency component of stimulation. The time integration was carried out using the second-order Crank-Nicolson method. The least-squares finite element approach was used with a reduced-order integration to ensure stability. The time-step size was 10 μs, and the problem was solved in the time domain for 5 ms (sufficient time to reach a periodical steady state). This time length was long enough to arrive at the periodic steady state. The mesh resolution for diffusion analysis was approximately 1 μm, resulting in about 225,000 first-order triangular elements. The initial time step was equal to the period of the stimulating frequency (1 ms) and was increased adaptively based on the convergence rate.

Data and codes availability

The data used in this study will be made available through a publicly accessible repository when accepted. The following temporary link contains the source codes to simulate **Fig. 5**. *https://figshare.com/s/600fc65f56587d473d48* When published, this private link will become public.

Funding

National Institute of Health NIDCD R01 DC020150 (PI: J-H Nam)

The funder had no role in study design, data collection and interpretation, or the decision to submit the work for publication.

Acknowledgements

The authors thank Jonathan Becker and Kris Abrams for their technical assistances.

Author contributions

CL, MS, and KSH contributed to this work equally. JHN, KSH, and LHC conceived and designed the experimental part of the study. JHN and MS conceived and designed the computational part of the study. KSH and CHL were the primary experimentalists who acquired experimental data. JHN, LHC and JCH participated in experiments. KHS wrote the codes to acquire data. JHN, KSH, LHC, and CHL analyzed experimental data. MS was the primary computational modeler. MS and JHN developed the computational analysis codes. MS simulated the computational codes. JHN drafted the MS and created the figures. JHN, MS, KSH, LHC, and JCH wrote the paper together.

Ethics

All experimental procedures were in accordance with NIH guidelines and approved by the University of Rochester Animal Care and Use Committee (protocol #: 101066).

References

Berg H. C. (1983) **Random walks in biology** Princeton, N.J: Princeton University Press

Berg H. C. (1993) **Random walks in biology** Princeton, N.J: Princeton University Press

Borkholder D. A., Zhu X., Frisina R. D. (2014) **Round window membrane intracochlear drug delivery enhanced by induced advection** *J Control Release* **174**:171–176

Cooper N. P., Vavakou A., van der Heijden M. (2018) **Vibration hotspots reveal longitudinal funneling of sound-evoked motion in the mammalian cochlea** *Nat Commun* **9**

Dewey J. B., Applegate B. E., Oghalai J. S. (2019) **Amplification and Suppression of Traveling Waves along the Mouse Organ of Corti: Evidence for Spatial Variation in the Longitudinal Coupling of Outer Hair Cell-Generated Forces** *J Neurosci* **39**:1805–1816

Dong W., Olson E. S. (2013) **Detection of cochlear amplification and its activation** *Biophys J* **105**:1067–1078

Fallah E., Strimbu C. E., Olson E. S. (2019) **Nonlinearity and amplification in cochlear responses to single and multi-tone stimuli** *Hear Res* **377**:271–281

Fettiplace R., Kim K. X. (2014) **The physiology of mechanoelectrical transduction channels in hearing** *Physiol Rev* **94**:951–986

Fisher J. A., Nin F., Reichenbach T., Uthaiah R. C., Hudspeth A. J. (2012) **The spatial pattern of cochlear amplification** *Neuron* **76**:989–997

Frisina R. D., Chamberlain S. C., Brachman M. L., Smith R. L. (1982) **Anatomy and physiology of the gerbil cochlear nucleus: an improved surgical approach for microelectrode studies** *Hear Res* **6**:259–275

Guinan J. J. (2022) **Cochlear amplification in the short-wave region by outer hair cells changing organ-of-Corti area to amplify the fluid traveling wave** *Hearing Research* **426**

He W., Burwood G., Porsov E. V., Fridberger A., Nuttall A. L., Ren T. (2022) **The reticular lamina and basilar membrane vibrations in the transverse direction in the basal turn of the living gerbil cochlea** *Sci Rep* **12**

He W., Kemp D., Ren T. (2018) **Timing of the reticular lamina and basilar membrane vibration in living gerbil cochleae** *Elife* **7**

Hirose K., Liberman M. C. (2003) **Lateral wall histopathology and endocochlear potential in the noise-damaged mouse cochlea** *J Assoc Res Otolaryngol* **4**:339–352

Jabeen T., Holt J. C., Becker J., Nam J. H. (2020) **Interactions between passive and active vibrations in the organ of Corti In vitro** *Biophysical Journal* **119**:314–325

Johnstone B. M., Patuzzi R., Syka J., Sykova E. (1989) **Stimulus-related potassium changes in the organ of Corti of guinea-pig** *J Physiol* **408**:77–92

Karavitaki K. D., Mountain D. C. (2007) **Evidence for outer hair cell driven oscillatory fluid flow in the tunnel of corti** *Biophys J* **92**:3284–3293

Lavigne P., Lavigne F., Saliba I. (2016) **Intratympanic corticosteroids injections: a systematic review of literature** *Eur Arch Otorhinolaryngol* **273**:2271–2278

Lee H. Y., Raphael P. D., Xia A., Kim J., Grillet N., Applegate B. E., Bowden A. K. Ellerbee, Oghalai J. S. (2016) **Two-Dimensional Cochlear Micromechanics Measured In Vivo Demonstrate Radial Tuning within the Mouse Organ of Corti** *J Neurosci* **36**:8160–8173

Lin W.-C., Macić A., Becker J., Nam J. H. (2024) **Asymmetric vibrations in the organ of Corti by outer hair cells measured from excised gerbil cochlea** *Commun Biol*

Liu Y., Gracewski S. M., Nam J. H. (2017) **Two passive mechanical conditions modulate power generation by the outer hair cells** *PLoS Comput Biol* **13**

Lukashkin A. N., Sadreev II, Zakharova N., Russell I. J., Yarin Y. M. (2020) **Local Drug Delivery to the Entire Cochlea without Breaching Its Boundaries** *iScience* **23**

Marnell D., Jabeen T., Nam J. H. (2018) **Hydrostatic measurement and finite element simulation of the compliance of the organ of Corti complex** *J Acoust Soc Am* **143**

Nam J. H. (2014) **Microstructures in the organ of Corti help outer hair cells form traveling waves along the cochlear coil** *Biophys J* **106**:2426–2433

Nam J. H., Fettiplace R. (2010) **Force transmission in the organ of Corti micromachine** *Biophys J* **98**:2813–2821

Nam J. H., Fettiplace R. (2012) **Optimal electrical properties of outer hair cells ensure cochlear amplification** *PLoS One* **7**

Nin F., Hibino H., Murakami S., Suzuki T., Hisa Y., Kurachi Y. (2012) **Computational model of a circulation current that controls electrochemical properties in the mammalian cochlea** *Proc Natl Acad Sci U S A* **109**:9191–9196

Ohyama K., Salt A. N., Thalmann R. (1988) **Volume flow rate of perilymph in the guinea-pig cochlea** *Hear Res* **35**:119–129

Olson E. S., Duifhuis H., Steele C. R. (2012) **Von Bekesy and cochlear mechanics** *Hear Res* **293**:31–43

Patuzzi R. (2011) **Ion flow in stria vascularis and the production and regulation of cochlear endolymph and the endolymphatic potential** *Hearing Research* **277**:4–19

Prodanovic S., Gracewski S. M., Nam J. H. (2019) **Power Dissipation in the Cochlea Can Enhance Frequency Selectivity** *Biophys J* **116**:1362–1375

Quraishi I. H., Raphael R. M. (2008) **Generation of the endocochlear potential: a biophysical model** *Biophys J* **94**:L64–66

Sadanaga M., Morimitsu T. (1995) **Development of endocochlear potential and its negative component in mouse cochlea** *Hear Res* **89**:155–161

Salt A. N., Hartsock J. J., Gill R. M., King E., Kraus F. B., Plontke S. K. (2016) **Perilymph pharmacokinetics of locally-applied gentamicin in the guinea pig** *Hear Res* **342**:101–111

Salt A. N., Hirose K. (2018) **Communication pathways to and from the inner ear and their contributions to drug delivery** *Hear Res* **362**:25–37

Salt A. N., Plontke S. K. (2005) **Local inner-ear drug delivery and pharmacokinetics** *Drug Discov Today* **10**:1299–1306

Salt A. N., Plontke S. K. (2018) **Pharmacokinetic principles in the inner ear: Influence of drug properties on intratympanic applications** *Hear Res* **368**:28–40

Salt A. N., Thalmann R., Marcus D. C., Bohne B. A. (1986) **Direct measurement of longitudinal endolymph flow rate in the guinea pig cochlea** *Hear Res* **23**:141–151

Schulte B. A., Schmiedt R. A. (1992) **Lateral wall Na,K-ATPase and endocochlear potentials decline with age in quiet-reared gerbils** *Hear Res* **61**:35–46

Shokrian M., Knox C., Kelley D. H., Nam J. H. (2020) **Mechanically facilitated micro-fluid mixing in the organ of Corti** *Sci Rep* **10**

Sun H., Hashino E., Ding D. L., Salvi R. J. (2001) **Reversible and irreversible damage to cochlear afferent neurons by kainic acid excitotoxicity** *J Comp Neurol* **430**:172–181

Szeto B., Chiang H., Valentini C., Yu M., Kysar J. W., Lalwani A. K. (2020) **Inner ear delivery: Challenges and opportunities** *Laryngoscope Investig Otolaryngol* **5**:122–131

Talaei S., Schnee M. E., Aaron K. A., Ricci A. J. (2019) **Dye Tracking Following Posterior Semicircular Canal or Round Window Membrane Injections Suggests a Role for the Cochlea Aqueduct in Modulating Distribution** *Front Cell Neurosci* **13**

Tandon V. *et al.* (2016) **Microfabricated reciprocating micropump for intracochlear drug delivery with integrated drug/fluid storage and electronically controlled dosing** *Lab Chip* **16**:829–846

Versteegh C. P., van der Heijden M. (2013) **The spatial buildup of compression and suppression in the mammalian cochlea** *J Assoc Res Otolaryngol* **14**:523–545

Wangemann P. (2006) **Supporting sensory transduction: cochlear fluid homeostasis and the endocochlear potential** *J Physiol* **576**:11–21

Wangemann P., Marcus D. C., Manley G. A., Gummer A. W. (2017) **Ion and fluid homeostasis in the cochlea** *Understanding the Cochlea* Cham: Springer :253–286

Zagadou B. F., Mountain D. C. (2012) **Analysis of the cochlear amplifier fluid pump hypothesis** *J Assoc Res Otolaryngol* **13**:185–197

Zhou W., Nam J. H. (2019) **Probing hair cell's mechano-transduction using two-tone suppression measurements** *Sci Rep* **9**

Zidanic M., Brownell W. E. (1990) **Fine structure of the intracochlear potential field. I. The silent current** *Biophys J* **57**:1253–1268

Author information

Choongheon Lee
Department of Otolaryngology, University of Rochester, Rochester, NY, United States

Mohammad Shokrian
Department of Mechanical Engineering, University of Rochester, Rochester, NY, United States

Kenneth S Henry
Department of Otolaryngology, University of Rochester, Rochester, NY, United States,
Department of Biomedical Engineering, University of Rochester, Rochester, NY, United States,
Department of Neuroscience, University of Rochester, Rochester, NY, United States
ORCID iD: 0000-0003-1364-318X

Laurel H Carney
Department of Biomedical Engineering, University of Rochester, Rochester, NY, United States,
Department of Otolaryngology, University of Rochester, Rochester, NY, United States,
Department of Neuroscience, University of Rochester, Rochester, NY, United States
ORCID iD: 0000-0002-4729-5702

Joseph C Holt
Department of Otolaryngology, University of Rochester, Rochester, NY, United States,
Department of Neuroscience, University of Rochester, Rochester, NY, United States
ORCID iD: 0000-0001-7908-083X

Jong-Hoon Nam
Department of Mechanical Engineering, University of Rochester, Rochester, NY, United States,
Department of Biomedical Engineering, University of Rochester, Rochester, NY, United States,
Department of Neuroscience, University of Rochester, Rochester, NY, United States
ORCID iD: 0000-0002-7477-5453

For correspondence: jong-hoon.nam@rochester.edu

Editors

Reviewing Editor
Catherine Carr
University of Maryland, College Park, United States of America

Senior Editor
Barbara Shinn-Cunningham
Carnegie Mellon University, Pittsburgh, United States of America

Reviewer #1 (Public review):

Summary:

The authors test the "OHC-fluid-pump" hypothesis by assaying the rates of kainic acid dispersal both in quiet and in cochleae stimulated by sounds of different levels and spectral content. The main result is that sound (and thus, presumably, OHC contractions and expansions) result in faster transport along the duct. OHC involvement is corroborated using

salicylate, which yielded results similar to silence. Especially interesting is the fact that some stimuli (e.g., tones) seem to provide better/faster pumping than others (e.g., noise), ostensibly due to the phase profile of the resulting cochlear traveling-wave response.

Strengths:

The experiments appear well controlled and the results are novel and interesting. Some elegant cochlear modeling that includes coupling between the organ of Corti and the surrounding fluid as well as advective flow supports the proposed mechanism.

The current limitations and future directions of the study, including possible experimental tests, extensions of the modeling work, and practical applications to drug delivery, are thoughtfully discussed.

Weaknesses:

Although the authors provide compelling evidence that OHC motility can usefully pump fluid, their claim (last sentence of the Abstract) that wideband OHC motility (i.e., motility in the "tail" region of the traveling wave) evolved for the purposes of circulating fluid---rather then emerging, say, as a happy by-product of OHC motility that evolved for other reasons---seems too strong.

https://doi.org/10.7554/eLife.101943.2.sa3

Reviewer #2 (Public review):

Although recent cochlear micromechanical measurements in living animals have shown that outer hair cells drive broadband vibration of the reticular lamina, the role of this vibration in cochlear fluid circulation remains unknown. The authors hypothesized that motile outer hair cells may facilitate cochlear fluid circulation. To test this hypothesis, they investigated the effects of acoustic stimuli and salicylate, an outer hair cell motility blocker, on kainic acid-induced changes in the cochlear nucleus activities. The results demonstrated that acoustic stimuli reduced the latency of the kainic acid effect, with low-frequency tones being more effective than broadband noise. Salicylate reduced the effect of acoustic stimuli on kainic acid-induced changes. The authors also developed a computational model to provide a physical framework for interpreting experimental results. Their combined experimental and simulated results indicate that broadband outer hair cell action serves to drive cochlear fluid circulation.

The major strengths of this study lie in its high significance and the synergistic use of electrophysiological recording of the cochlear nucleus responses alongside computational modeling. Cochlear outer hair cells have long been believed to be responsible for the exceptional sensitivity, sharp tuning, and huge dynamic range of mammalian hearing. However, recent observations of the broadband reticular lamina vibration contradict widely accepted view of frequency-specific cochlear amplification. Furthermore, there is currently no effective noninvasive method to deliver the drugs or genes to the cochlea, a crucial need for treating sensorineural hearing loss, one of the most common auditory disorders. This study addresses these important questions by observing outer hair cells' roles in the cochlear transport of kainic acid. The well-established electrophysiological method used to record cochlear nucleus responses produced valuable new data, and the custom-developed developed computational model greatly enhanced the interpretation of the experimental results.

The authors successfully tested their hypothesis, with both the experimental and modeling results supporting the conclusion that active outer hair cells can enhance cochlear fluid circulation in the living cochlea.

The findings from this study can potentially be applied for treating sensorineural hearing loss and advance our understanding of how outer hair cells contribute to cochlear amplification and normal hearing.

https://doi.org/10.7554/eLife.101943.2.sa2

Reviewer #3 (Public review):

Summary:

This study reveals that sound exposure enhances drug delivery to the cochlea through the non-selective action of outer hair cells. The efficiency of sound-facilitated drug delivery is reduced when outer hair cell motility is inhibited. Additionally, low-frequency tones were found to be more effective than broadband noise for targeting substances to the cochlear apex. Computational model simulations support these findings.

Strengths:

The study provides compelling evidence that the broad action of outer hair cells is crucial for cochlear fluid circulation, offering a novel perspective on their function beyond frequency-selective amplification. Furthermore, these results could offer potential strategies for targeting and optimizing drug delivery throughout the cochlear spiral.

Weaknesses:

The primary weakness of this paper lies in the surgical procedure used for drug administration through the round window. Opening the cochlea can alter intracochlear pressure and disrupt the traveling wave from sound, a key factor influencing outer hair cell activity. However, the authors do not provide sufficient details on how they managed this issue during surgery. Additionally, the introduction section needs further development to better explain the background and emphasize the significance of the work.

Comments on revisions:

Thank you for addressing the comments and concerns. The author has responded to all points thoroughly and clarified them well. However, please include the key points from the responses to the comments (Introduction ((3), (5)) and Results ((5)) into the manuscript. While the explanations in the response letter are reasonable, the current descriptions in the manuscript may limit the reader's understanding. Expanding on these points in the Introduction, Results, or Discussion sections would enhance clarity and comprehensiveness.

https://doi.org/10.7554/eLife.101943.2.sa1

Author response:

The following is the authors' response to the original reviews.

> ***Public Reviews:***
>
> ***Reviewer #1 (Public review):***
>
> *Summary:*
>
> *The authors test the "OHC-fluid-pump" hypothesis by assaying the rates of kainic acid dispersal both in quiet and in cochleae stimulated by sounds of different levels and*

> *spectral content. The main result is that sound (and thus, presumably, OHC contractions and expansions) results in faster transport along the duct. OHC involvement is corroborated using salicylate, which yielded results similar to silence. Especially interesting is the fact that some stimuli (e.g. tones) seem to provide better/faster pumping than others (e.g. noise), ostensibly due to the phase profile of the resulting cochlear traveling-wave response.*
>
> *Strengths:*
>
> *The experiments appear well controlled and the results are novel and interesting. Some elegant cochlear modeling that includes coupling between the organ of Corti and the surrounding fluid as well as advective flow supports the proposed mechanism.*
>
> *Weaknesses:*
>
> *It's not clear whether the effect size (e.g., the speed of sound-induced pumping relative to silence) is large enough to have important practical applications (e.g., for drug delivery). The authors should comment on the practical requirements and limitations.*

With our current data, what we can conclude is that modest sound levels (e.g., 75 dB SPL noise or an 80 dB SPL tone) facilitates cochlear drug delivery. We added a paragraph to the Discussion stating some future considerations for application to drug delivery in the human cochlea.

> *Although helpful so far as it goes, the modeling could be taken much further to help understand some of the more interesting aspects of the data and to obtain testable predictions. In particular, the authors should systematically explore the level effects they find experimentally and determine whether the model can replicate the finding that different sounds produce different results (e.g. noise vs tone).*
>
> *The model should also be used to relate the model's flow rates more quantitatively to the properties of the traveling wave (e.g., its phase profile).*

The present study is focused on explaining the principle of mass transport in the cochlea. The quantification of the relationship between flow rate and traveling wave is an important open question and will be the topic of future studies. Our previous modeling study (Shokrian et al. 2020) showed a clear relation between the traveling wave characteristics (e.g., amplitude and phase velocity) and the mass transport in the Corti fluid. As the reviewer correctly pointed out, the current paper is focused on designing controlled experiments to provide proof of concept along with computational simulations to support our major claim (that outer hair cells stir cochlear fluid).

> *Finally, the model should be used to investigate differences between active and passive OHCs (e.g., simulating the salicylate experiment by disabling the model's OHCs).*

What the reviewer asks for has been demonstrated in previous theoretical studies (Lighthill, 1992; Edom, Obrist, Kleiser, 2014; Sumner, Reichenbach, 2021). In some of the previous studies, it was called the steady streaming. These studies are excellent examples because they simulated the sensitive cochlea (similar level of basilar membrane vibrations) but did not incorporate the Corti fluid peristalsis. Even without the peristaltic motion of the Corti tube, the basilar membrane-scala fluid interaction generated steady streaming (creepy fluid flow). However, the streaming velocity of cochlear models without active peristalsis along the Corti tube is about three orders of magnitude smaller than the active cochlea at a comparable level of basilar membrane vibrations. For example, the peak streaming speed was < 0.1 um/s at 80 dB SPL, and it took > 4 hours for particles to travel 1 mm. This speed is much slower than the particle transport speed due to pure diffusion (Sumner, Reichenbach, 2021).

> *The manuscript would be stronger if the authors discussed ways to test their hypothesis that OHC motility serves a protective effect by pumping fluid. For example, do animals held in quiet after noise exposure (TTS) take longer to recover?*

We agree with the reviewer. The following statements were added to the Discussion section. “Our results have implications for cochlear fluid homeostasis. For example, future studies can test the hypothesis that an acoustically rich environment would be beneficial in maintaining healthy hearing as well as in recovering from transient hearing loss.”

> ***Reviewer #2 (Public review):***
>
> *Summary:*
>
> *Recent cochlear micromechanical measurements in living animals demonstrated outer hair celldriven broadband vibration of the reticular lamina that contradicts frequency-selective cochlear amplification. The authors hypothesized that motile outer hair cells can drive cochlear fluid circulation. This hypothesis was tested by observing the effects of acoustic stimuli and salicylate, an outer hair cell motility blocker, on kainic acid-induced changes in the cochlear nucleus activities. It was found that acoustic stimuli can reduce the latency of the kainic acid effect, and a low-frequency tone is more effective than broadband noise. Salicylate reduced the effect of acoustic stimuli on kainic acid-induced changes. The authors also developed a computational model to provide the physical basis for interpreting experimental results. It was concluded that experimental data and simulations coherently indicate that broadband outer hair cell action is for cochlear fluid circulation.*
>
> *Strengths:*
>
> *The major strengths of this study include its high significance and the combination of electrophysiological recording of the cochlear nucleus responses with computational modeling. Cochlear outer hair cells have been believed to be responsible for the exceptional sensitivity, sharp tuning, and huge dynamic range of mammalian hearing. Recent observation of the broadband reticular lamina vibration contradicts frequency-specific cochlear amplification. Moreover, there is no effective noninvasive approach to deliver the drugs or genes to the cochlea for treating sensorineural hearing loss, one of the most common auditory disorders. These important questions were addressed in this study by observing outer hair cells' roles in the cochlear transport of kainic acid. The well-established electrophysiological method for recording cochlear nucleus responses produced valuable new data, and the purposely developed computational model significantly enhanced the interpretation of the data.*
>
> *The authors successfully tested their hypothesis, and both the experimental and modeling results support the conclusion that active outer hair cells can drive cochlear fluid circulation in the living cochlea.*
>
> *Findings from this study will help auditory scientists understand how the outer hair cells contribute to cochlear amplification and normal hearing.*

We thank the reviewer for acknowledging our effort.

> *Weaknesses:*
>
> *While the statement "The present study provides new insights into the nonselective outer hair cell action (in the second paragraph of Discussion)" is well supported by the results, the authors should consider providing a prediction or speculation of how this hair cell*

> *action enhances cochlear sensitivity. Such discussion would help the readers better understand the significance of the current work.*

We added a potential implication to the Discussion, that an acoustically rich environment could be beneficial in maintaining healthy hearing as well as recovering from damaged hearing.

> ***Reviewer #3 (Public review):***
>
> *Summary:*
>
> *This study reveals that sound exposure enhances drug delivery to the cochlea through the nonselective action of outer hair cells. The efficiency of sound-facilitated drug delivery is reduced when outer hair cell motility is inhibited. Additionally, low-frequency tones were found to be more effective than broadband noise for targeting substances to the cochlear apex. Computational model simulations support these findings.*
>
> *Strengths:*
>
> *The study provides compelling evidence that the broad action of outer hair cells is crucial for cochlear fluid circulation, offering a novel perspective on their function beyond frequency-selective amplification. Furthermore, these results could offer potential strategies for targeting and optimizing drug delivery throughout the cochlear spiral.*
>
> *Weaknesses:*
>
> *The primary weakness of this paper lies in the surgical procedure used for drug administration through the round window. Opening the cochlea can alter intracochlear pressure and disrupt the traveling wave from sound, a key factor influencing outer hair cell activity. However, the authors do not provide sufficient details on how they managed this issue during surgery. Additionally, the introduction section needs further development to better explain the background and emphasize the significance of the work.*

Although we wrote that the inner ear left intact, it might have not been sufficiently clear. Our surgical approach leaves the inner ear intact, including the round-window membrane. The round window in gerbil is concave like a bowl. We applied 4 μL of kainic acid solution in the round-window niche, without perforating the round-window membrane.

> ***Recommendations For The Authors:***
>
> ***Reviewer #1 (Recommendations for the authors):***
>
> *The authors' choice to frame their findings by hinting that they have discovered the "real" reason for the evolution of broadband OHC electromotility (e.g., the first and last sentences of the abstract and parts of the Discussion), although clearly intended to boost the perceived significance of the work, does them no favors and will probably lead to distracting criticisms they could easily have avoided. The manuscript would be significantly improved by removing or downplaying these rather speculative and unsupported claims; the work stands on its own without them.*

We agree that the first line of the Abstract might distract the readers. Meanwhile, in the Discussion, we believe the readers will appreciate our speculation of how this study is relevant to recent debates on hearing mechanics. Following the reviewer's advice, we have revised the Abstract.

> ***Reviewer #3 (Recommendations for the authors):***
>
> *Please review the detailed comments below. I hope they contribute to enhancing the paper:*

We thank the reviewer for this detailed advice. All of these comments make good sense and were very helpful in improving this paper or in planning future studies.

Many of the comments were relevant to the computer model, and they have one common basis, which we have not yet achieved. I.e., simulating the level-dependence.

> *I. Introduction*
>
> *(1) Please clarify and improve this sentence. Effective and safe strategies for delivering treatments to the inner ear have been reported: 'Consequently, intervening in hearing health by delivering substances to the inner-ear fluid is challenging'.*

The preceding statement is regarding the blood-labyrinthine barrier (BLB), comparable to the bloodbrain barrier (BBB). We revised the statement: “Consequently, intervening in hearing health by delivering substances to the inner-ear fluid through systemic circulation is challenging.”

> *(2) Please expand on how the secretion and absorption of ions and molecules maintain the unique ionic compositions of the two intracochlear fluids. Include details on the role of the stria vascularis and the specific functions of the three types of strial cells in this process.*

In response to this request, we added a paragraph discussing cochlear fluid homeostasis. Our study is different from existing homeostasis studies in three regards. First, the site: Existing studies are centered on the stria vascularis, while this study concerns the Corti fluid. Second, the mechanism: Existing studies are regarding metabolic transport, while our scope is the transport due to fluid flow. Third, the range: Existing studies considered local electrochemical equilibrium within a radial section, while this study concerns global (longitudinal) mass transport. To address this comment, the following was added to the Discussion.

“Our study complements existing studies regarding cochlear fluid homeostasis and differs from previous studies in several ways. The intrastrial fluids (extracellular fluids in the stria vascularis) have been more thoroughly investigated because the three layers in the stria vascularis (marginal, intermediate, and basal cells) maintain the endocochlear potential (Wangemann 2006).

Equilibrium in the Corti fluid has been sparsely investigated because its electrochemical gradient is modest compared to that of the intrastrial fluids (Johnstone, Patuzzi et al. 1989; Zidanic and Brownell 1990). Local electrochemical balance in the cochlear fluids has been considered within a radial section (Quraishi and Raphael 2008; Patuzzi 2011; Nin, Hibino et al. 2012). Our study is focused on the longitudinal (global) equilibrium along the cochlear coil and did not consider the equilibrium across the stria vascularis cell layers. To examine whether the longitudinal fluid flow driven by outer hair cells is strong enough to affect cochlear fluid homeostasis, future studies should measure the K^+ equilibrium and recycling along the length of the Corti fluid under sound and silence conditions.“

> *(3) Please provide a more detailed explanation and definition of a longitudinal electrochemical gradient, including how it functions and its relevance in physiological processes.*

The most researched electrochemical gradient of the cochlea must be the endocochlear potential that varies along the cochlear length. The endocochlear potential at any location is determined by the equilibrium between the source and the sink. In the view of the Corti fluid, the source is the potassium current out of the hair cells and the sink is the resorption of potassium by supporting cells. The effect of a longitudinal electrochemical gradient on hearing physiology is beyond the scope of this study. To do so would require incorporating detailed K+ equilibrium dynamics. This certainly is one of our future directions.

> *(4) Please include the necessary references to support these three sentences: "Diffusion is an effective mechanism for a substance to travel along submicrometer distances. For instance, it takes microseconds for neurotransmitters to diffuse across a 20-nm synaptic gap. In contrast, diffusion is inefficient for travel on the centimeter scale. It takes days for a drug applied at the round window to travel 30 mm to the apical end of the human cochlea. In practice, the substance would not reach the apex because it would be resorbed before traveling the distance".*

A reference was added (Berg, 1993). Our description of diffusion is based on the fundamental physics of Fick's laws.

> *(5) In paragraph 3, the author only discussed a portion of the previous approaches. There are numerous methods for inner ear delivery, including external, middle ear, and direct inner ear delivery via the round window or semicircular canal. Each method has its pros and cons, which the authors should carefully address. For example, the semicircular canal approach doesn't require two perforations in the inner ear and distributes the injection evenly throughout the cochlea.*

A recent review paper regarding inner ear drug delivery was added as a reference (Szeto, Chiang et al. 2020). Drug delivery is a means to demonstrate the OHC's role in longitudinal mass transport. We are concerned that comparing different drug delivery modalities in detail would distract the readers from the main point of this study. We mentioned 'one remedy' with two perforations, for which abundant case studies are found in the literature. Discussing existing approaches exhaustively can be better done by review papers.

> *(6) The following sentence is inaccurate and should be carefully rephrased. Previous reports chose higher volumes than the actual fluid volume to maximize the drug (or gene) effect, but this was not a requirement of the delivery methods: 'Such an invasive approach requires the injection of a substantial fluid volume, larger than the entire perilymph in the inner ear'.*

We revised the statement to relax the wording 'require': 'Such an invasive approach is often associated with the injection of a substantial fluid volume, larger than the entire perilymph in the inner ear (Szeto, Chiang et al. 2020)'. This statement might be acceptable because we found few invasive delivery papers that used < 1 μL. Moreover, the physics basis of the injection method is to replace the fluid in a labyrinth compartment with a new fluid (a good example where this fluid physics was tested with quantitative data is the Lichtenhan et al. 2016 paper).

> *(7) Please provide the necessary references. Also, clarify what is meant by 'actuator cells'. Are you referring to hair cells?: 'The tube-shaped organ of Corti (OoC) is lined with actuator cells and the cells are activated systematically with a large phase velocity (> a few m/s) toward the apex'.*

Yes, we meant OHCs as the actuator cells. This point has been clarified. A reference for the phase velocity has been added (Olson, Duifhuis, Steele, 2012).

> *II. Results*
>
> *(1) Is there a specific reason you use 60 or 75 dB SPL for broadband sounds, but opt for louder sounds (80 dB SPL) for pure tones?*

It is not straightforward to compare the SPL between broadband noise and a pure tone, and we did not attempt to 'equate' them in any way.

> *(2) Please provide specific details about the sound generation protocol, including the duration, start time, end time, and any other relevant parameters. Here is an example of a vague sentence. Do you play the sounds continuously during these time periods, or only at specific intervals?: 'In two example cases, the effect time at low-CF locations (CFs near 2 kHz) was 15 minutes for the case of the 0.5 kHz tone (Fig. 3A)'*

It is described in the Measurement protocol part of the Methods section (see the red text below). In the exampled case and all other cases, the sounds were played continually (not continuously).

For the "Sound" protocol, 1.1-s noise pips (60 or 75 dB SPL, 0.1-12 kHz bandwidth, 0.8-s duration including 0.15-s onset/offset ramps) were presented continually. After 48 noise pips, one 1.1-s silent pause and three CF tone pips followed (a total of 51 pips and a pause make a 57.2-s sequence). The CF tone pips were presented at the level of 35 dB SPL to monitor neural responses. The silence pause was to monitor spontaneous neural responses. The sequence was repeated until neural signals at the lowest CF site were completely abolished. The neural responses presented in this study are the 'driven responses' obtained by subtracting the spontaneous responses from the responses to the 35 dB CF tones. For the "Silence" or "Pure-tone" protocol, the noise pips of the Sound protocol were replaced with either silence pauses or a pure tone at 80 dB SPL.

> *(3) Providing a schematic timeline of your experiments indicating sound generation, kainic acid (and salicylate) application, as well as DPOAE and AVCN recordings would greatly help in understanding and following your results.*

We have revised Figure 2.

> *(4) How did you control the opening(s) for the injection? The openings could alter intracochlear pressure and affect the traveling wave from the sound, which is the major factor influencing outer hair cell activity.*

We did not open the inner ear. The round window remained intact. Opening the bulla does not affect the intracochlear pressure. We have clarified this issue, beginning with the first sentence of the Abstract. Thanks for raising this important question.

> *(5) Is there any reason why the author generated only low and mid-frequencies? If so, please address what the limitations were in testing high frequency.*

There are no limitations to testing high frequencies. High frequencies would not affect drug delivery to the apex of the cochlea because the traveling waves stop right after the CF location. We are interested in delivering drugs deeper into the apex. Our presented results support this reasoning: mid-frequency stimulation was less effective for delivery to the low CF location.

> *(6) I suggest combining Figures 3E and 3F to facilitate a direct comparison between the Silence and Noise conditions, as the MF and LF plots are overlapping in these panels.*

We considered this change but realized that it might introduce confusion and difficulty in parsing the results. Moreover, the two panels have their respective messages.

> *(7) In Figure 3E, why does the LF tone affect both Low and Mid CFs, while the MF tone only affects Mid CF?*

The cochlear traveling wave stops right after the CF location. Peristaltic action takes place in the broad tail region of the traveling waves (see Fig. 5C).

> *III. Materials and Methods*
>
> *(1) Please provide details about your injection protocol. Did you create additional perforations? How did you target the round window? What was the injection rate? How did you seal the round window, and so on?*

The inner ear including the round window was left intact. Only the bulla was open.

> *(2) Please include details about your surgical procedure for the AVCN recording, including probe insertion.*

AVCN recording is a well-established technique. Instead of reintroducing the method, we added a classical reference with friendlier description (Frisina, Chamberlain, et al., 1982).

> *IV. Minor points*
>
> *(1) Please include the full terms for the abbreviations 'CF', 'DPOAEs', 'PT', 'IP', and 'RW' for readers who are not in the hearing research field.*

We have checked that these abbreviations were defined.

> *(2) Are 'GXXX's in figures animal identifiers? Please clarify what they represent.*

Yes, they are animal identifiers. We have clarified this point in Fig. 1 caption.

https://doi.org/10.7554/eLife.101943.2.sa0